ACOUSTICS 2012

Bayesian sparse regularization in near-field wideband aeroacoustic imaging for wind tunnel test

N. Chu[a], J. Picheral[b] and A. Djafari[a]

[a]Laboratoire des signaux et systèmes, 3 rue Joliot-Curie, 91192 Gif Sur Yvette, France, Metropolitan

[b]Supelec, Département Signaux & Systèmes, 91192 Gif-sur-Yvette, France

ning.chu@lss.supelec.fr

Robust deconvolution-based methods using sparsity constraint and sparse regularization achieve high spatial resolutions in aeroacoustic imaging in low Signal-to-Noise Ratio (SNR). But sparse prior and model parameters should be further optimized to obtain super resolution and be robust to sparsity constraint. In this paper, we propose a Robust Approach with Bayesian Sparse Regularization in Aeroacoustic Imaging (RABSRAI) to detect both positions and powers of near-field wideband uncorrelated sources in poor SNR case, and simultaneously estimate background noise. The Bayesian interpretation is applied to select the sparse prior and regularization parameter in stead of knowing source number or SNR. On simulated and wind tunnel data, proposed approach is compared with the beamforming, DAMAS, Diagonal Remove DAMAS, Robust DAMAS with sparsity constraint (SC-RDAMAS), Covariance Matrix Fitting (CMF) and CLEAN.

1 Introduction

Nowadays aeroacoustic imaging has become a standard technique for mapping the location and strength of aeroacoustic sources with microphone arrays. It provides insight into noise generating mechanisms, which is used for designing quieter vehicles and machinery. In this paper, we aim to investigate near-field wideband aeroacoustic imaging on vehicle surface in wind tunnel test based on the 2D Non-Uniform microphone Array (NUA). The beamforming method is simple and fast, but its spatial resolution and dynamic range are limited due to high sidelobes. The MUSIC greatly improves resolutions, but its resolution requires high SNR and source number. Though the Near-field Acoustic Hologram (NAH) provides good resolution over entire frequency band, but it is limited by hologram size and can not work well with sparse antenna array. The CLEAN [8] iteratively extracts peak sources from a beamforming image, but it could not separate sources from severe noises. The Deconvolution Approach for Mapping of Acoustic Source (DAMAS) method [1] becomes a breakthrough and is successfully applied in wind tunnel test, however, it is sensitive to noise and suffers from slow convergence. The DAMAS2 and DAMAS3 accelerate the DAMAS by using the invariant point spread function (PSF) which inevitably harms resolutions. The Covariance Matrix Fitting (CMF) method [9] works better than the above, but is not feasible to use it due to its huge variable dimensionality. Recently the Robust DAMAS with Sparse Constraint (SC-RDAMAS) [2] achieves super spatial resolution and estimates noise variance, but sparsity constraint on total source power is hard to determine in poor SNR. Above all, most of classical methods suffers at least one of these drawbacks: poor spatial resolutions, sensitive to background noise, need for source number and high computational cost.

To overcome most of above drawbacks, proposed approach is to exploit the sparsity of source spatial distributions by applying Bayesian framework. Our novelties are that we apply Double Exponential model as spatial sparse prior to obtain super resolutions in poor SNR, and with the help of Bayesian interpretation, regularization parameter is determined based on the forward model error and prior model parameter. By comparing with the state-of-art methods on simulations and real data, the advantages of proposed approach are robust to noise, super resolution, wide dynamic range of power estimations and feasible to use in near-field wideband aeroacoustic source imaging for vehicle surface in wind tunnel test based on 2D NUA array.

This paper is organized as follows: In Section 2, formulation of aeroacoustic imaging is briefly introduced. Then our approach is proposed in Section 3. Performance comparisons on simulations and real data are illustrated in Section 4 and Section 5. Finally conclusions are made in Section 6.

2 Formulation of aeroacoustic imaging

2.1 Assumptions

Four necessary assumptions are made: Sources are punctual, temporally uncorrelated; noise is Additive Gaussian White Noise (AGWN), independent and identically distributed (iid); sensors are omnidirectional with unitary gain; and reverberations could be negligible in the anechoic wind tunnel.

2.2 Forward propagation model

Consider M antenna sensors and K near-field wideband sources $\boldsymbol{s}^* = [s_1^*, \cdots, s_K^*]$. And the scanning plane consists of N ($N >> M > K$) scanning points $\boldsymbol{s} = [s_1, \cdots, s_N]^T$ at positions $\boldsymbol{p} = [\boldsymbol{p}_1, \cdots, \boldsymbol{p}_N]^T$ with $\boldsymbol{p}_n$ being 3D coordinate of the point n. Each scanning point could be regarded as a potential source. The total snapshots T_0 of each sensor is divided into T segments, where each segment consists of L snapshots. Each segment is then converted into L narrow frequency bins by Discrete Fourier Transform. Thus for the segment $i \in [1, T]$ and single frequency f_l, $l \in [1, L]$, the observed vector $\boldsymbol{z}_i(f_l) = [z_{i1}(f_l), \cdots, z_{iM}(f_l)]^T$ at antenna array is modeled:

$$\boldsymbol{z}_i(f_l) = \boldsymbol{A}(\boldsymbol{p}, f_l)\boldsymbol{s}_i(f_l) + \boldsymbol{e}_i(f_l) \tag{1}$$

where $\boldsymbol{e}_i(f_l) = [e_{i1}(f_l), \cdots, e_{iM}(f_l)]^T$ denotes the AGWN noise, and $\boldsymbol{A}(\boldsymbol{p}, f_l) = [\boldsymbol{a}(\boldsymbol{p}_1, f_l), \cdots, \boldsymbol{a}(\boldsymbol{p}_N, f_l)]$ is $M \times N$ near-field steering matrix, with steering vector:

$$\boldsymbol{a}(\boldsymbol{p}_n, f_l) = [\frac{1}{r_{n,1}} e^{-j2\pi f_l \tau_{n,1}}, \cdots, \frac{1}{r_{n,M}} e^{-j2\pi f_l \tau_{n,M}}]^T \tag{2}$$

where $\tau_{m,n}$ is the propagation time from the source n to antenna m, and $r_{n,m}$ is the propagation distance during $\tau_{m,n}$. Actual $r_{n,m}$ and $\tau_{n,m}$ will be corrected according to the refraction in the wind tunnel in Section 5.

2.3 Classical inverse solutions

2.3.1 Near-field beamforming

For the given location $\boldsymbol{p}_n$ and single frequency f_l, the steering vector $\boldsymbol{a}(\boldsymbol{p}_n, f_l)$ is short as $\boldsymbol{a}_n$. An estimate of source power y_n locating at the scanning point n can be obtained by the beamforming as:

$$y_n = \frac{\tilde{\boldsymbol{a}}_n^H \hat{\boldsymbol{R}} \tilde{\boldsymbol{a}}_n}{\|\tilde{\boldsymbol{a}}_n\|^2} \tag{3}$$

where operator $(\cdot)^H$ denotes the conjugate transpose; $\|\cdot\|$ is the vector norm; and the beamforming coefficient $\tilde{\boldsymbol{a}}_n$ is:

$$\tilde{\boldsymbol{a}}_n = [r_{n,1} e^{-j2\pi f_l \tau_{n,1}}, \cdots, r_{n,M} e^{-j2\pi f_l \tau_{n,M}}]^T \tag{4}$$

and $\hat{\boldsymbol{R}} = \frac{1}{T}\sum_{i=1}^{T} \boldsymbol{z}_i(f_l)\boldsymbol{z}_i(f_l)^H$ is the estimation of observed covariance matrix $\boldsymbol{R}$, with $\boldsymbol{R}$ being modeled into:

$$\boldsymbol{R} = E\{\boldsymbol{z}_i(f_l)\boldsymbol{z}_i(f_l)^H\} = \boldsymbol{A}\boldsymbol{X}\boldsymbol{A}^H + \sigma^2\boldsymbol{I} \tag{5}$$

where σ^2 is the noise variance; $\boldsymbol{I}$ is the identical matrix; operator $E\{\cdot\}$ denotes the mathematical expectation; and $\boldsymbol{X} = E\{\boldsymbol{s}\boldsymbol{s}^H\}$ is the source correlation matrix, which is diagonal for uncorrelated sources with $\boldsymbol{x} = diag(\boldsymbol{X})$ standing for source power vector.

2.3.2 DAMAS [1] and its improved methods

When total snapshot segment is large enough $T >> 1$, we get $\hat{\boldsymbol{R}} \approx \boldsymbol{R}$. By neglecting noise in Eq.(5), the DAMAS [1] method is deduced as:

$$\boldsymbol{y} = \boldsymbol{C}\boldsymbol{x} \tag{6}$$

where $\boldsymbol{x} = [x_1, \cdots, x_N]^T$; $\boldsymbol{y} = [y_1, \cdots, y_N]^T$, and power transferring matrix $\boldsymbol{C}$ has the coefficient (PSF) $c_{n,q} = \frac{\|\bar{\boldsymbol{a}}_n^H \boldsymbol{a}_q\|^2}{\|\bar{\boldsymbol{a}}_n\|^2}$ with $n, q = 1, \cdots, N$. Its iterative non-negative solution is:

$$\hat{x}_n = y_n - \left[\sum_{q=1}^{n-1} c_{nq}\hat{x}_q + \sum_{q=n+1}^{N} c_{nq}\hat{x}_q\right], \quad \hat{x}_n \geq 0 \tag{7}$$

The DAMAS is a powerful technique to deconvolve the beamforming result. However, the biggest drawback is that it is not robust to noise pollution. Several methods improve its robustness. Diagonal Removal (DR) DAMAS [1] constrains $diag\{\hat{R}\} = 0$ to suppress noise interference, but DR technique harms weak sources; instead of deconvolving the beamforming result, the CMF with sparsity constraint [9] directly estimates observed covariance matrix $\boldsymbol{R}$ and noise variance σ^2, however, its variable matrix is too large to solve, so the CMF converges very slowly; the SC-RDAMAS method [2] estimates the noise variance to improve robustness, and applies sparsity constraint on total source power to achieve super spatial resolutions, but sparsity constraint is not easily determined in very poor SNR.

3 Proposed approach

3.1 Bayesian sparse regularization

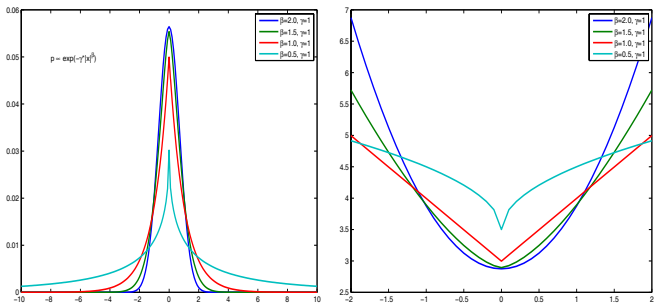

(a) Probability density function $\mathcal{GG}(\boldsymbol{x})$ (b) $-ln[\mathcal{GG}(\boldsymbol{x})]$ function

Figure 1: Generalized Gaussian family

Sparsity fact reveals that sources sparsely lay out on object surface, and the source number is rather fewer than the scanning points. Many literatures have explored sparse distribution prior such as discussed in [7]. For monopole sources, we select a distribution with a sharp summit and short tail among Generalized Gaussian family $\mathcal{GG}(x)$ with respect to ℓ_1 regularization. For uncorrelated centralized variable x, the prior model based on $\mathcal{GG}(x)$ is expressed:

$$p(\boldsymbol{x}) = \prod_n^N \mathcal{GG}(x_n|\gamma,\beta) \propto \exp\left[-\gamma\sum_n^N |x_n|^\beta\right] \tag{8}$$

where probability density function (PDF) of $\mathcal{GG}(x_n|\gamma,\beta)$ is

$$\mathcal{GG}(x_n|\gamma,\beta) = \frac{\beta\gamma}{2\Gamma(1/\beta)}\exp\left[-\gamma|x_n|^\beta\right] \tag{9}$$

where $\Gamma(\cdot)$ represents the Gamma function, and γ and β control PDF pattern. Particularly, when $\beta = 1$, we get the Double Exponential $\mathcal{DE}(x)$ model as:

$$p(\boldsymbol{x}) = \prod_n^N \mathcal{DE}(x_n|\gamma) \quad \propto \quad \exp\left[-\gamma\|\boldsymbol{x}\|_1\right] \tag{10}$$

Four examples of $\mathcal{GG}(\boldsymbol{x})$ family and their $-ln[\mathcal{GG}(\boldsymbol{x})]$ functions are illustrated on Figure 1. For cases $0 < \beta < 1$, it is of great interest to enforce sparsity, but its $-ln[\mathcal{GG}(\boldsymbol{x})]$ function is not convex. The Double Exponential model is sparse enough, and its $-ln[\mathcal{GG}(\boldsymbol{x})]$ function is convex. For source powers $\boldsymbol{x}$, non-negative condition is combined with Double Exponential prior.

After determining source spatial distribution prior, we consider the likelihood $p(\boldsymbol{y}|\boldsymbol{x},\sigma^2)$. In forward propagation model of Eq.(1), the system error $\xi = [\xi_1, \cdots, \xi_N]$ is modeled by:

$$\xi = \boldsymbol{y} - \boldsymbol{C}\boldsymbol{x} - \sigma^2\boldsymbol{1}_N \tag{11}$$

ξ denotes the residue part, who consists of estimation errors and unpredictable parts in forward model. Generally ξ is supposed to be Gaussian $\xi \sim \mathcal{N}(0, \sigma_\xi^2)$. Thus the likelihood $p(\boldsymbol{y}|\boldsymbol{x},\sigma^2)$ is deduced into:

$$p(\boldsymbol{y}|\boldsymbol{x},\sigma^2) = \frac{1}{(2\pi\sigma_\xi^2)^{N/2}}\exp\left[-\frac{\|\boldsymbol{y} - \boldsymbol{C}\boldsymbol{x} - \sigma^2\boldsymbol{1}_N\|^2}{2\sigma_\xi^2}\right] \tag{12}$$

According to the Bayes' rule, the Joint Maximum A Posteriori (JMAP) criterion is expressed as:

$$\mathcal{J}_{JMAP}(\boldsymbol{x},\sigma^2) = -ln[p(\boldsymbol{y}|\boldsymbol{x},\sigma^2)p(\boldsymbol{x})p(\sigma^2)] \tag{13}$$

For simplicity, we take Jeffreys prior for $p(\sigma^2) \sim \frac{1}{\sigma^2}$. Substituting Eq.(10) and Eq.(12) into Eq.(13), we get JMAP criterion by omitting small terms as follows:

$$\mathcal{J}_{JMAP}(\boldsymbol{x},\sigma^2) \propto \|\boldsymbol{y} - \boldsymbol{C}\boldsymbol{x} - \sigma^2\boldsymbol{1}_N\|^2 + \alpha\|\boldsymbol{x}\|_1 \tag{14}$$

Where regularization parameter is

$$\alpha = 2\sigma_\xi^2\gamma \tag{15}$$

with

$$\sigma_\xi^2 = Tr(\hat{R}) - \|\boldsymbol{x}\|_1 - M\sigma^2 \tag{16}$$

where $Tr(\hat{R})$ denotes total power of observed signals. When σ^2 becomes bigger, $Tr(\hat{R})$ consequently increases and σ_ξ^2 is inevitably lager. Due to power conservation, equation (16) means that the residual power σ_ξ^2 equals the total received power minus original source powers and noise power. Therefore regularization parameter α is the function of $\|\boldsymbol{x}\|_1$ and

σ^2. Moreover, equation (14) means that larger the system error σ_ξ^2 is, less accurate the forward model becomes, therefore the more we need to enforce sparse distribution prior by increasing α. Generally ℓ_1-norm for enforcing sparsity and noise variance estimation are discussed in many literatures such as [3] and [4]. However, instead of source number estimation or subspace separation, we apply the Bayesian frame to jointly estimate the source power $\boldsymbol{x}$ and noise variance σ^2. The Eq.(14) is a convex criterion and can be solved alternatively for x and σ^2. In our proposed approach in Eq.(14), the Bayesian interpretation is applied to select proper sparse prior to enforce ponctuel sources and achieve super spatial resolution, and the regularization parameter is inherently determined without knowing exact SNR or source number.

3.2 Wideband estimation

In wind tunnel experiment, aeroacoustic sources are generated by the friction and collision between the car and wind flow. Physically, different car parts with various sizes produce vibrations with different frequencies. Therefore aeroacoustic sources are near-field wideband signals. Consider the frequency range $[f_{min}, f_{max}]$ consisting of L frequency bins. Let $\hat{\boldsymbol{x}}(f_l)$ be the estimation of $\boldsymbol{x}(f_l)$ in lth frequency bin. Then source powers $\boldsymbol{x}_{wb}$ over wideband $[f_{min}, f_{max}]$ can be estimated by $\hat{\boldsymbol{x}}_{wb} = \frac{1}{L}\sum_{f_l=f_{min}}^{f_{max}} \hat{\boldsymbol{x}}(f_l)$.

4 Simulation

In this part, we compare proposed approach with some of the state-of-art methods in strong background noise ($SNR = 0dB$) based on real wind tunnel configurations at single frequency $f = 2500Hz$. There are 64 2D NUA array on vertical plane, whose averaging array aperture is $d = 2m$ with longer horizontal aperture, as shown in Figure 4a. For NUA array, it yields almost the same performance as the uniform array with more sensors does as discussed in [5]. The distance between source plane and array is around $R = 4.50m$, thus the beamforming resolution at $f = 2500Hz$ is $\Delta B \approx \lambda R/d = 31cm$. For scanning step, we choose $\Delta x = 5cm$ to satisfy $\Delta x/\Delta B < 0.2$ for any $f < 3500Hz$, which avoids the spatial aliasing in the DAMAS [1]. The propagation speed is $c_0 \approx 340m/s$. Results are illustrated by decibel (dB) images and section profiles.

In Figure 3a, five uncorrelated complex sources ($K = 5$) are spaced $15cm - 20cm$ ($3-4$ pixels) from the center source, as shown in Figure 3a. Their source powers are from -9.71 to $4.27dB$ ($x_1^* < x_2^* < \cdots < x_5^*$) with $14dB$ dynamic range. The background noise variance is $-1.25dB$ ($\sigma^2 = 0.75$), and the averaging $SNR = 0dB$.

Figure 3 shows that the beamforming just gets a very confused image due to its low resolutions at $2500Hz$; the DAMAS fails to distinguish weak sources due to its sensitivity to noise; the DR-DAMAS detects strong sources and removes the noise interference, but it also eliminates weak source; the CLEAN gets better spatial resolutions, but still sensitive to noise; the CMF well estimates the noise variance and finds out all sources, but its resolutions are not high enough; the SC-RDAMAS works faster and better than the CMF, but proposed approach outperforms the others. It not only better locates all sources, but also well estimates noise variance. In the proposed approach, $\gamma = 1$ in $\mathcal{DE}(x)$ model is selected as Figure 1a shown. And the influence of regularization parameter in $SNR = 0$ are shown in Figure 2: thanks to noise estimation, proposed approach can achieve relatively small power image reconstruction error δ_2 even if α is very small. As shown in Table 1, proposed approach has the minimal averaging power estimation error $\overline{\Delta x^*} = \frac{1}{K}\|\hat{\boldsymbol{x}}^*_k - \boldsymbol{x}^*_k\|_1$ with $\boldsymbol{x}^* = diag\{E[\boldsymbol{s}^*\boldsymbol{s}^{*H}]\}$ and $\delta_2 = \frac{\|\boldsymbol{x}-\hat{\boldsymbol{x}}\|^2}{\|\boldsymbol{x}\|^2}$.

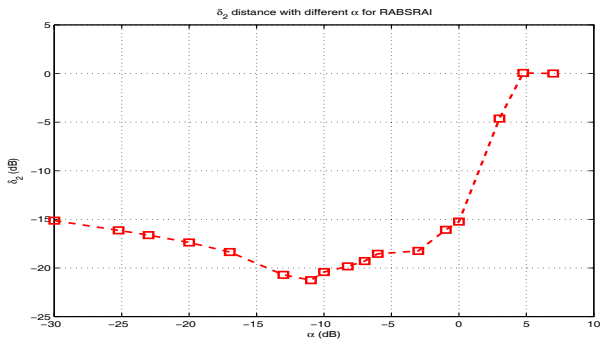

Figure 2: Regularization parameter influence in proposed approach, power image reconstruction error $\delta_2 = \frac{\|\boldsymbol{x}-\hat{\boldsymbol{x}}\|^2}{\|\boldsymbol{x}\|^2}$

Table 1: Power estimation error and noise variance estimation $\hat{\sigma^2}$.

Powers	x_1^*	x_2^*	x_3^*	x_4^*	x_5^*	$\overline{\Delta x^*}$	δ_2	$\hat{\sigma^2}$
Beamforming	9.30	7.57	1.49	1.02	0.45	3.97	115	-
CLEAN	4.24	1.36	2.98	0.52	0.12	1.80	1.46	-
DAMAS	1.00	1.00	1.00	1.00	0.30	0.86	0.06	-
DR-DAMAS	1.00	0.44	0.14	0.10	0.11	0.36	0.03	-
CMF	0.48	0.35	0.23	0.22	0.26	0.31	0.09	0.74
SC-RDAMAS	0.54	0.45	0.09	0.08	0.12	0.26	0.02	0.74
Proposed	0.32	0.43	0.09	0.02	0.07	0.19	0.01	0.75

5 Real data

Figure 4 shows configurations of wind tunnel S2A [6]. The scanning region is $135\times470cm^2$. There are $T_0 = 524288$ snapshots, $T = 204$ segments, $L = 2560$ snapshots per segment. Wideband is $2400Hz - 2600Hz$ with $B = 21$ frequency bins. The results are shown by normalized dB images with $10dB$ span. For corrections of propagation time $\tau_{n,m}$ and distance $r_{n,m}$, we apply equivalent source that antenna m seems to receive the signal from equivalent source n' along a direct line $d_{n',m}$ during the same propagation time $\tau_{n',m}$, as if there is no wind influence, as shown in Figure 4b.

After corrections, Figure 5a illustrates that the beamforming just gives an fuzzy image of strong sources around the front wheel, rearview mirror and back wheel; in Figure 5b, the DAMAS greatly improve spatial resolutions of the beamforming result, however it gets many false targets in the air; the DR-DAMAMS well eliminates most of false targets, but it envitably removes weak sources on the front light, front cover, and side windows; Figure 5d shows that the CLEAN overcomes drawbacks of the DAMAS and DR-DAMAS, but unexpected strong points are detected on the ground; in Figure 5e, the SC-RDAMAS obtains a result as good as the

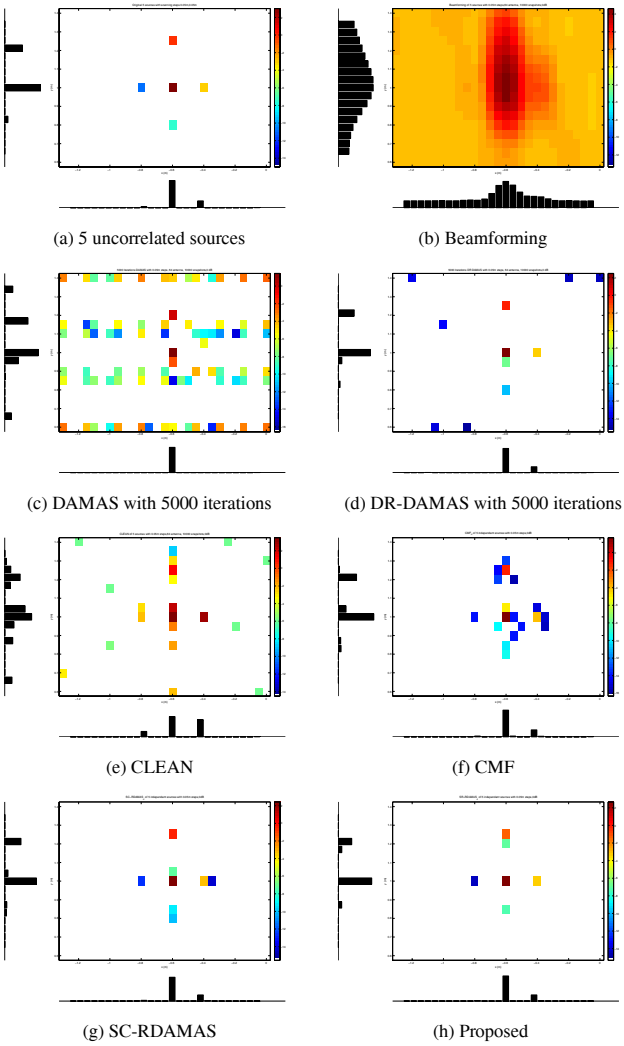

(a) 5 uncorrelated sources (b) Beamforming

(c) DAMAS with 5000 iterations (d) DR-DAMAS with 5000 iterations

(e) CLEAN (f) CMF

(g) SC-RDAMAS (h) Proposed

Figure 3: Acoustic imaging of 17×27 pixels $2500Hz$ under the conditions of background noise $\sigma^2 = 0.75$, averaging $SNR = 0dB$ and dynamic range $14dB$.

CLEAN, but false alarms under the car body are still so many; Figure 5f shows the proposed approach not only suppress the noise and obtain more precise power levels and positions than the above methods, but also discovers weak sources around two wheels and the mirror, as well as removes most of false targets under the cars and in the air.

Figure 6 illustrates the detail of rear mirror part. Consistently in previous simulation, the beamforming just gives 3 strong sources with narrow dynamic range of powers; the DAMAS improves the resolutions, but unexpected interference could not be removed; the DR-DAMAS overcomes strong interference, but the resolutions on rear mirror are not high enough; the CMF and SC-RDAMAS achieve almost the same

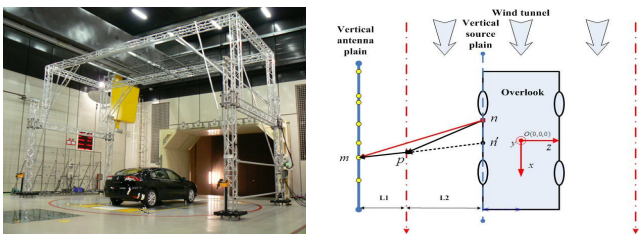

(a) Wind tunnel S2A [6]. (b) Overlook and wind tunnel effect.

Figure 4: Configurations of wind tunnel S2A.

results, much better than the above; but some interferences are still existing; fortunately proposed approach clearly removes unexpected false alarms and better detects sources around rear mirror and on the front wheel with wide dynamic range as color map shown in Figure 6f.

Based on the effectiveness at single frequency, we give the comparisons on wideband data at $2400 - 2600Hz$, as Figure 7 illustrated. Each method obtains a better result than the corresponding in Figure 5, since the real sources are enforced and the flashing false targets are suppressed over the wideband average. Above all, proposed approach in Figure 7d enforces the sparse distribution and extracts more accurate source positions and powers both for the strong sources around the front wheel and weak ones on the mirror and back wheel.

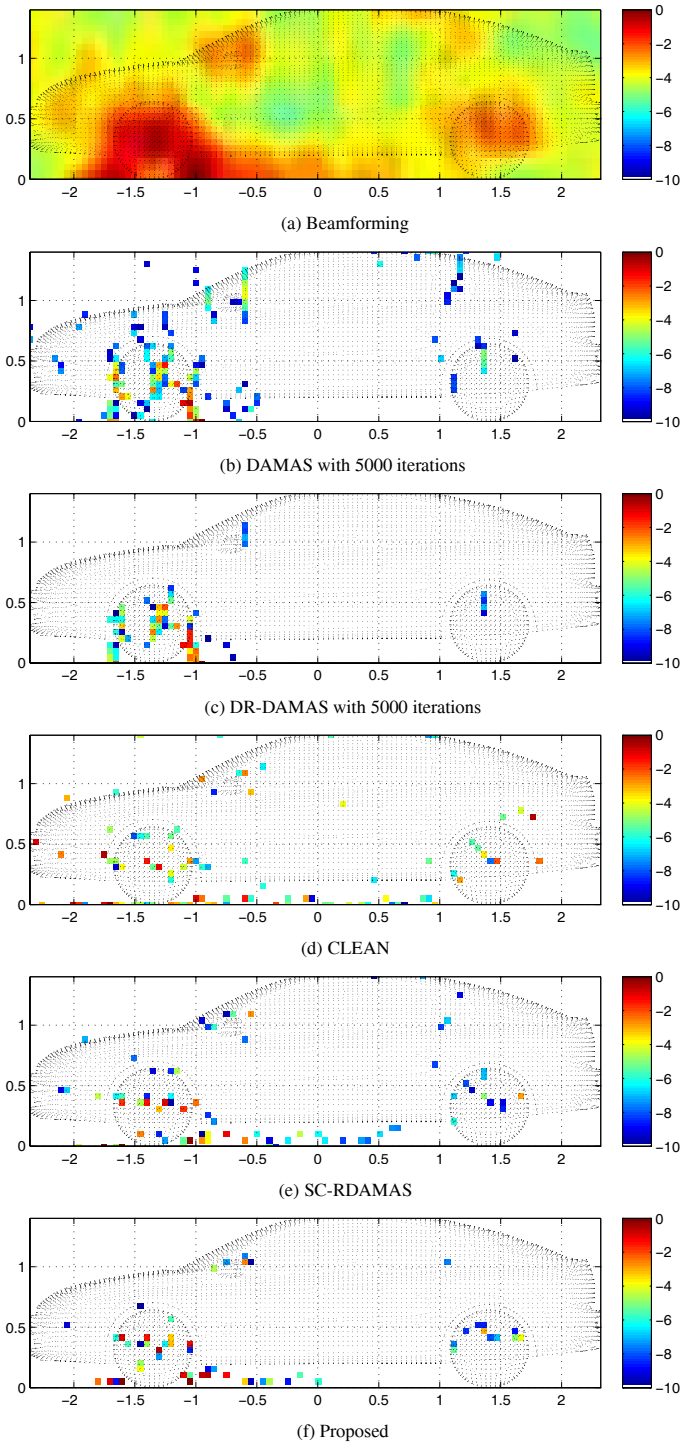

(a) Beamforming

(b) DAMAS with 5000 iterations

(c) DR-DAMAS with 5000 iterations

(d) CLEAN

(e) SC-RDAMAS

(f) Proposed

Figure 5: Whole vehicle at $f = 2500Hz$, $10dB$ span.

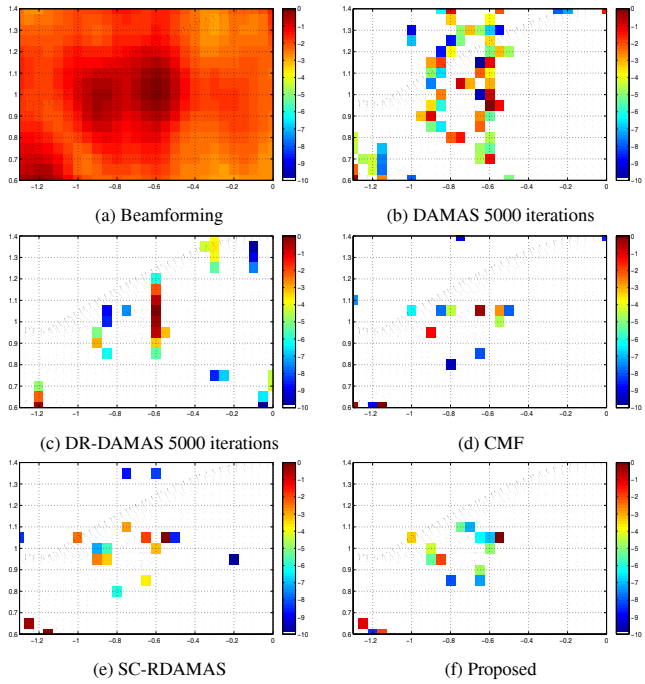

(a) Beamforming (b) DAMAS 5000 iterations (c) DR-DAMAS 5000 iterations (d) CMF (e) SC-RDAMAS (f) Proposed

Figure 6: Rearview mirror part at $f = 2500Hz$, $10dB$ span

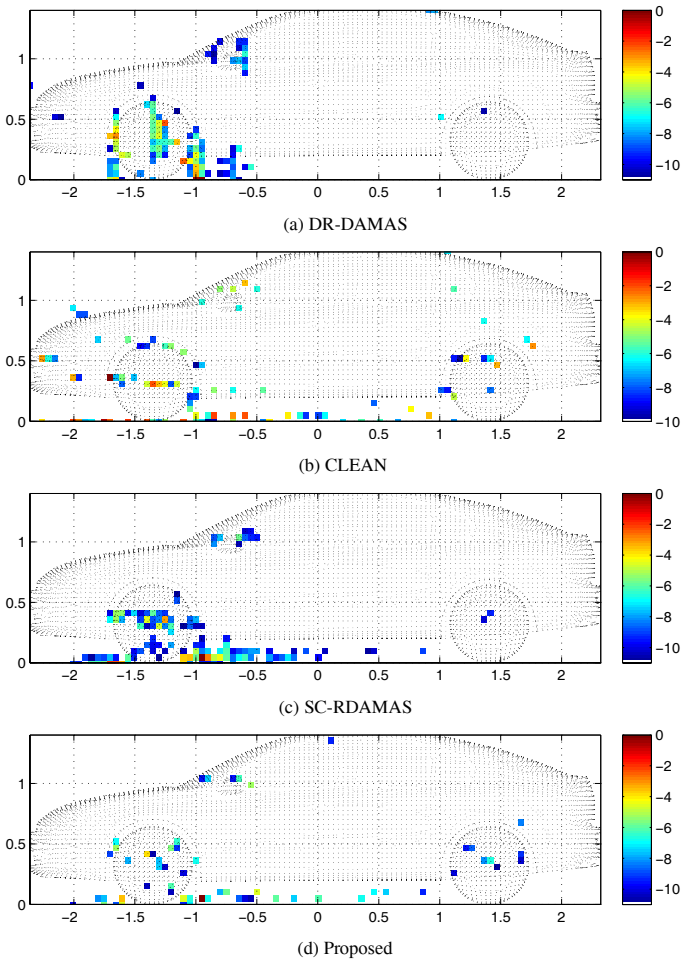

(a) DR-DAMAS (b) CLEAN (c) SC-RDAMAS (d) Proposed

Figure 7: Wideband data over $f \in [2400, 2600]Hz$, $10dB$ span

6 Conclusions

We propose a Robust Approach with Bayesian Sparse Regularization in Aeroacoustic Imaging (RABSRAI) to detect positions and powers of near-field wideband uncorrelated sources in poor SNR case, and simultaneously estimate background noise. Bayesian interpretation is investigated for sparse spatial distribution prior and regularization parameter without knowing source number or SNR. The advantages of our method are robust to noise, wide dynamic range of power estimation, super resolutions and feasible to use based on 2D NUA array in wind tunnel test. Proposed method is compared with the state-of-art methods on simulations and experiment data. For future works, we are investigating a Bayesian inference approach to adaptively estimate hyperparameter in forward model and prior models.

Acknowledgment

Authors gratefully thank Renault SAS for offering real data and their valuable suggestions.

References

[1] T.F. Brooks and W.M. Humphreys. A deconvolution approach for the mapping of acoustic sources (DAMAS) determined from phased microphone arrays. *Journal of Sound and Vibration*, 294(4-5):856–879, 2006.

[2] N. CHU, J. Picheral, and A. M. Djafari. A robust super-resolution approach with sparsity constraint for near-field wideband acoustic imaging. In *IEEE International Symposium on Signal Processing and Information Technology*, pages 286–289, Bilbao, Spain, Dec.14-17,2011.

[3] D. Malioutov et al. A sparse signal reconstruction perspective for source localization with sensor arrays. *IEEE Transactions on Signal Processing*, 53(8):3010–3022, 2005.

[4] Nicolas P. Galatsanos and Aggelos K. Katsaggelos. Methords for choosing the regularization parameters and estimating the noise variance in image restoration and thier relation. *IEEE Transactions on Image Processing*, 1(3):332–336, 1992.

[5] Carine El Kassis, José Picheral, and Chafic Mokbel. Advantages of nonuniform arrays using root-music. *Signal Processing*, pages 689–695, 2010.

[6] Arnaud Menoret, Nathalie Gorilliot, and Jean-Luc Adam. Imagerie acoustique en soufflerie S2A. In Société Française d'Acoustique SFA, editor, *10ème Congrès Français d Acoustique*, Lyon, France, 2010.

[7] Ali Mohammad-Djafari. Bayesian approach with prior models which enforce sparsity in signal and image processing. *EURASIP Journal on Advances in Signal Processing*, Special issue on Sparse Signal Processing, 2012.

[8] P. Sijtsma. Clean based on spatial source coherence. *International Journal of Aeroacoustics*, 6(4):357–374, 2007.

[9] Tarik Yardibi, Jian Li, Petre Stoica, Nikolas S. Zawodny, and Louis N. Cattafesta. A covariance fitting approach for correlated acoustic source mapping. *Journal of The Acoustical Society of America*, 127, 2010.